Time-frequency analysis of long fiber Bragg gratings with low reflectivity

Juan Sancho,[1] Sanghoon Chin,[2*] David Barrera,[1] Salvador Sales,[1] and Luc Thévenaz[2]

[1]*iTEAM Institute, Universidad Politécnica de Valencia, 46022 Valencia, Spain*
[2]*Ecole Polytechnique Fédérale de Lausanne, Institute of Electrical Engineering, SCI-STI-LT Station 11, 1015 Lausanne, Switzerland*
[*]*sanghoon.chin@gmail.com*

Abstract: A new technique to investigate the spatial distribution of the reflection spectrum along fabricated long weak fiber Bragg gratings (FBG) is experimentally demonstrated, together with its potential applications for distributed fiber sensing and broadband signal processing. A short pulsed coherent light signal is launched into a FBG and the signal frequency is scanned through the FBG reflection spectrum. When the pulse duration is set much shorter than the transit time through the grating a time-resolved reflected signal can be obtained for each signal frequency. It informs about the distribution of the refractive index periodic perturbation along the entire FBG length, hence the uniformity or frequency chirp information of the fabricated FBG. This technique has been implemented to demonstrate a distributed temperature sensing system with high spatial resolution and to also realize a robust all-fiber tunable delay line for broadband signals.

OCIS codes: (060.3735) Fiber Bragg gratings; (060.2370) Fiber optics sensors; (230.1480) Bragg reflectors;

References and links

1. A. D. Kersey, M. A. Davis, H. J. Patrick, M. LeBlanc, K. P. Koo, C. G. Askins, M. A. Putnam, and E. J. Friebele, "Fiber Grating Sensors," J. Lightwave Technol. **15**(8), 1442–1463 (1997).
2. W. F. Liu, I. M. Liu, L. W. Chung, D. W. Huang, and C. C. Yang, "Acoustic-induced switching of the reflection wavelength in a fiber Bragg grating," Opt. Lett. **25**(18), 1319–1321 (2000).
3. J. Azaña, "Proposal of a uniform fiber Bragg grating as an ultrafast all-optical integrator," Opt. Lett. **33**(1), 4–6 (2008).
4. I. Littler, M. Rochette, and B. Eggleton, "Adjustable bandwidth dispersionless bandpass FBG optical filter," Opt. Express **13**(9), 3397–3407 (2005).
5. M. Volanthen, H. Geiger, and J. P. Dakin, "Distributed grating sensors using low-coherence reflectometry," J. Lightwave Technol. **15**(11), 2076–2082 (1997).
6. H. Murayama, H. Igawa, K. Kageyama, K. Ohta, I. Ohsawa, K. Uzawa, M. Kanai, T. Kasai, and I. Yamaguchi, "Distributed strain measurement with high spatial resolution using fiber Bragg gratings and optical frequency domain reflectometry," in *Optical Fiber Sensors*, OSA Technical Digest (CD) (Optical Society of America, 2006), paper ThE40.
7. K. Hotate and K. Kajiwara, "Proposal and experimental verification of Bragg wavelength distribution measurement within a long-length FBG by synthesis of optical coherence function," Opt. Express **16**(11), 7881–7887 (2008).
8. L. R. Chen, S. D. Benjamin, P. W. E. Smith, and J. E. Sipe, "Ultrashort pulse reflection from fiber gratings: a numerical investigation," J. Lightwave Technol. **15**(8), 1503–1512 (1997).
9. J. Azaña and M. A. Muriel, "Study of optical pulses-fiber gratings interaction by means of joint time-frequency signal representations," J. Lightwave Technol. **21**(11), 2931–2941 (2003).
10. N. J. Doran and D. Wood, "Nonlinear-optical loop mirror," Opt. Lett. **13**(1), 56–58 (1988).
11. L. Thévenaz and M. A. Soto, "Rating the performance of a Brillouin distributed fiber sensor," 22nd *OFS2012*, Proc. SPIE **8421**, 8421A7 (2012).
12. S. Chin, N. Primerov, and L. Thevenaz, "Sub-centimeter spatial resolution in distributed fiber sensing based on dynamic Brillouin grating in optical fibers," Sensors Journal, IEEE **12**(1), 189–194 (2012).
13. K. Y. Song, Z. He, and K. Hotate, "Distributed strain measurement with millimeter-order spatial resolution based on Brillouin optical correlation domain analysis," Opt. Lett. **31**(17), 2526–2528 (2006).
14. L. Thevenaz, S. Foaleng Mafang, and J. Lin, "Impact of pump depletion on the determination of the Brillouin gain frequency in distributed fiber sensors," Proc. SPIE 7753, *21st International Conference on Optical Fiber Sensors*, 775322 (2011).

#183098 - $15.00 USD Received 8 Jan 2013; revised 4 Mar 2013; accepted 5 Mar 2013; published 14 Mar 2013

15. M. Lancry and B. Poumellec, "UV laser processing and multiphoton absorption processes in optical telecommunication fiber materials," Phys. Rep. **523**(4), 207–229 (2013).

1. Introduction

Fiber Bragg gratings (FBGs) are considered as key devices in fiber optic-based signal processing systems due to their simplicity, low insertion loss, polarization independence, low cost and their full compatibility with fiber optics systems. For these reasons, FBGs have been extensively implemented for many potential applications such as sensors [1], switches [2], temporal integrators [3] and filters [4]. Several methods have been proposed to characterize the Bragg-frequency distribution along FBGs [5–7], based on optical low-coherence reflectometry and optical frequency domain reflectometry. However, both techniques show a limited measurement range and a slow response and require very complicated setup. Another approach based on synthesis of optical coherence function (SOCF) seems to be promising since a section along the long FBG can selected to be interrogated and its position can be reconfigured by simply tuning the modulation frequency of the light source. So, the grating properties can be characterized point by point, yet with a complex measurement setup. Numerical study on time or time-frequency analysis of FBGs have been demonstrated, based on the impulse response and spectrograms [8, 9].

In this paper, we propose and experimentally demonstrate a new technique to measure the distribution of central frequency of a long weak FBG, based on time-frequency domain analysis. The measurement system is essentially based on the principle of optical time domain reflectometry (OTDR) while performing a step-wise scan of the frequency of the interrogating pulse, therefore reducing the complexity of the instrumentation and drastically simplifying the measurement layout. In addition, this type of FBG-based optical time-frequency domain reflectometry has been successfully implemented to develop a distributed sensing system with sub-centimeter spatial resolution and to realize a continuously tunable delay line for broadband optical signals. A simple estimation clearly demonstrates that such a scheme can offer an attractive and effective solution to realize a new class of distributed fiber sensors, provided that the technological challenge to imprint a very weak uniform FBG along long lengths of fiber can be overcome.

2. Principle of operation

The principle of operation to characterize the central frequency distribution of a long FBG with low reflectivity is depicted in Fig. 1. An optical pulse with duration much shorter than the propagation time through the FBG is used as interrogating signal and sent into the grating through an optical circulator. Due to the low reflectivity of the grating, a tiny fraction of the signal pulse will experience a back-reflection along the entire length of the grating during propagation. Then the continuously back-scattered wave takes the typical square waveform, as shown in Fig. 1(a), with a duration determined by the grating length and equal to the doubled transit time through the grating [8]. The spectrum of this backscattered waveform is essentially given by the product of the incident signal spectrum with the overall grating reflection spectrum. In a time domain interpretation the impulse response of the grating – that maps all longitudinal variations of the local reflectivity – is convolved with the interrogating

#183098 - $15.00 USD Received 8 Jan 2013; revised 4 Mar 2013; accepted 5 Mar 2013; published 14 Mar 2013

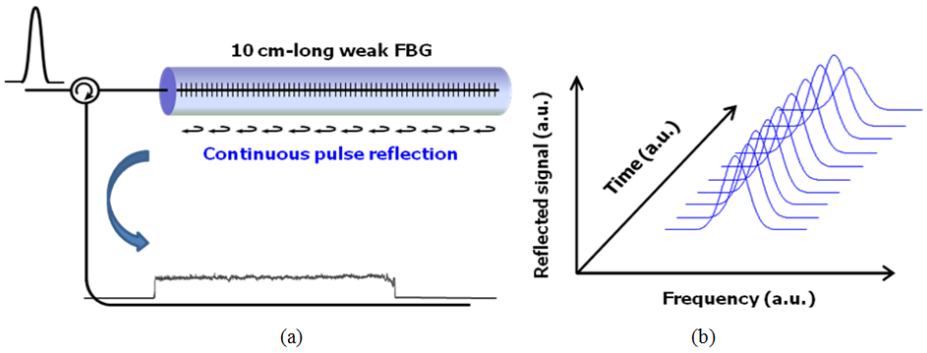

Fig. 1. (a) Schematic diagram of operation principle to characterize optical properties of a long and weak FBG in distributed manner. (b) Time-frequency response of the FBG.

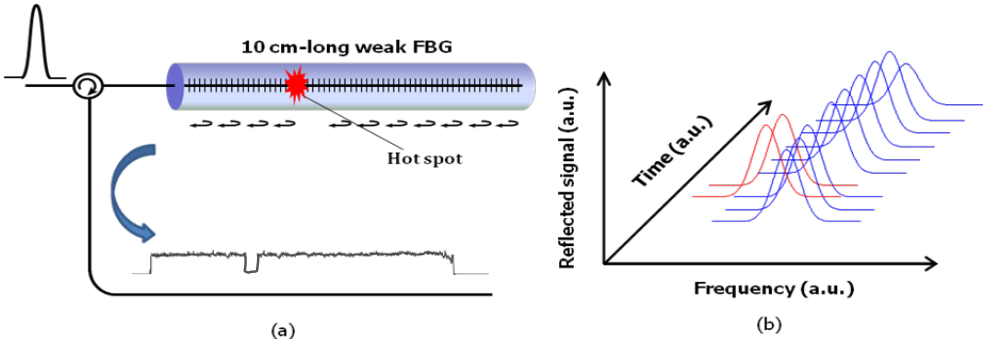

Fig. 2. Schematic diagram of operation principle to characterize optical properties of a long and weak FBG in distributed manner when a hot spot is inserted. (b) Time-frequency response of the FBG.

pulse waveform. Therefore, for a fixed signal frequency the amplitude variation of the back-scattered wave can be attributed to local variations of the grating structure if the interrogating pulse duration is much shorter than the typical length of these variations. The distribution of FBG reflection spectrum can be readily interrogated by simply scanning the signal frequency of the interrogating pulse in the vicinity of the grating resonance frequency, as shown in Fig. 1(b). Then the retrieved spectrum can be analyzed and straightforwardly transposed in a mapping of the refractive index variation along the FBG. Figure 2(a) illustrates the effect of a local perturbation along the grating, i.e. caused by a temperature change at a given position. Such perturbation leads to a variation in the refractive index and thus to a spectral shift of the peak frequency at that position in the time-frequency response, as sketched in Fig. 2(b).

Figure 3 shows the simulated time-frequency response of the FBG subject to such an interrogating signal. The FBG used in the simulation is 10 cm-long and uniform, showing a global reflection spectrum with a FWHM spectral width of about 1 GHz, and an overall reflectivity limited to 35%. A 20 ps Gaussian-shaped pulse is used as interrogating pulse. The amplitude of the reflected signal is calculated through the inverse Fourier Transform of the product between the input pulse spectrum and the FBG reflection spectrum. By simply mapping the temporal waveform of the signal reflection as a function of the central frequency of the interrogating pulse, a time-frequency analysis of the FBG can be obtained, as shown in Fig. 3(a). As expected, the amplitude of the back-reflection decreases slightly over the distance due to the gradual depletion of the incident pulse during propagation, as a result of the weak but non-zero distributed reflection. To illustrate a distributed sensing situation, Fig. 3(b) shows the calculated time-frequency mapping when a 5 mm-long hot spot at 25 K above room temperature is positioned at the center of the grating. The temperature shift modifies the

#183098 - $15.00 USD Received 8 Jan 2013; revised 4 Mar 2013; accepted 5 Mar 2013; published 14 Mar 2013

refractive index profile along the limited section of the grating where the hot spot is placed. Consequently, the peak frequency of the local reflection spectrum at that position will be spectrally shifted by an amount determined by the thermal response of the FBG.

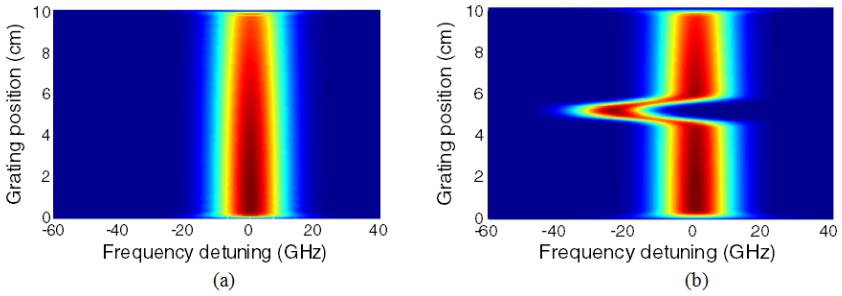

Fig. 3. Numerical simulation result of 3D-distribution of the FBG spectrum along a 10 cm-long weak FBG (a) when the grating is uniform (b) in the presence of a 5 mm-long hot spot.

3. Experimental setup for sensing applications

A schematic diagram of the experimental setup is represented in Fig. 4. A 10-cm long FBG was home fabricated to validate the concept of the proposed measurement system. The optical properties of the FBG were measured using a broadband light source, showing an overall reflectivity of 35% and a central wavelength at 1549 nm with a FWHM spectral width of 1.7 GHz. In addition, the thermal response of the peak frequency of the grating was measured to be −1.23 GHz/K. A commercial distributed-feedback (DFB) laser diode was used as a light source. Its output was connected to an external fast electro-optic modulator (EOM), so that its intensity could be shaped as a Gaussian pulse with 40 ps FWHM duration. The pulse repetition rate was set to 2 ns, equivalent to the transit time through a 40 cm optical fiber, so that the absence of overlapping between backscattered signals from successive pulses is secured. The signal pulse was then delivered to a nonlinear optical loop mirror, in order to eliminate any DC background component in the generated pulse, since any possible interference noise caused by a CW reflection can impair the measurement dynamic range. As a side benefit, the intensity dependence of the nonlinear loop mirror transmission resulted in a temporally compressed output pulse down to 20 ps FWHM [10]. So, the spectral distribution of the FBG reflection could be measured with a 2 mm spatial resolution. An optical isolator was placed at the output of the grating to suppress any unwanted back reflection from the end facet of the fiber.

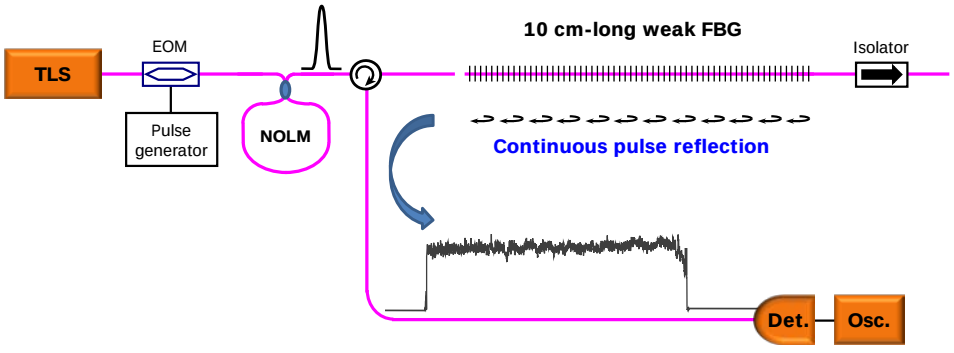

Fig. 4. Experimental layout to measure the distributed reflection spectrum of a 10 cm-long FBG with overall reflectivity of 35%.

#183098 - $15.00 USD Received 8 Jan 2013; revised 4 Mar 2013; accepted 5 Mar 2013; published 14 Mar 2013

To conveniently measure the variation of the refractive index along the FBG, the laser frequency was precisely tuned by controlling the injection current applied to the laser diode while the ambient temperature around the FBG was preserved and no strain was applied to the FBG. Then the pulse reflection was monitored by scanning step-by-step the central frequency of the signal pulse, by a step of 250 MHz over a span of 125 GHz. Considering the effective reflection bandwidth of 22 GHz, the reflection spectrum was sampled by 88 points, which gives enough accuracy to determine the peak frequency of the reflected spectrum with a good precision [11]. The time waveform at each step was acquired without averaging using a sampling oscilloscope with a 80 GHz optical module. Figure 5(a) and Fig. 5(b) show the measured 3D distribution of the reflected power of the weak FBG and the distribution of the FBG peak frequency, respectively, by simply plotting the frequency at which the peak reflection of the incident signal pulse is estimated. It can be clearly observed that the FBG frequency is slightly chirped at the beginning and at the end of the long grating, which could be attributed to the imperfections in the fabrication process. Nevertheless, it can be considered that the FBG was fairly uniformly written along its 10 cm length.

To validate the concept of the distributed sensing scheme using FBG-based time-frequency domain analysis, an 8 mm-long hot spot at 25 K above room temperature was placed near the beginning of the grating. Figures 6(a) and 6(b) depict the 3D map of the FBG time-frequency measurements and the retrieved FBG frequency distribution, respectively. As expected, the local spectrum at the test position was down-shifted by –31 GHz, corresponding to the previously measured thermal response of the FBG. Therefore, it confirms the high potential of this type of distributed sensing system based on a long and weak FBG. Actually, the principle to realize distributed sensing is conceptually similar to other time-domain distributed sensing systems, such as Brillouin-based fiber sensors [12, 13]. However, this system presents crucial advantages: no need of optical pumping to generate a temporary reflecting grating along the sensing fiber since the FBG is static in fiber and the reflection process is passive. As a consequence, the grating reflecting strength is not determined by the interrogating pulse energy, unlike in Brillouin based system in which the grating is dynamically generated by the interrogating pulse. This sets less restriction to the achievement of extreme spatial resolution systems.

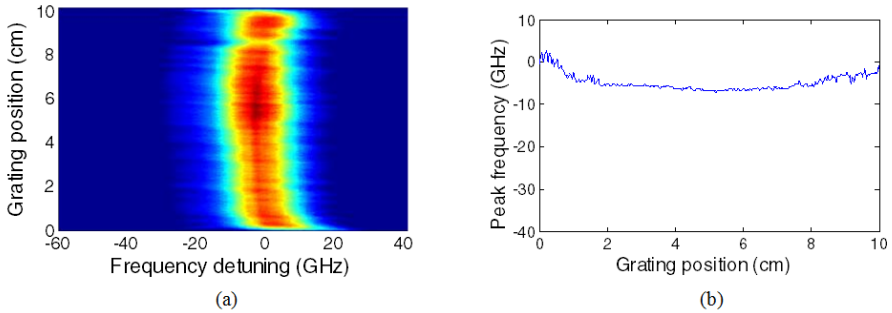

Fig. 5. (a) Measured 3D-map of the reflected power of the FBG with no change in temperature and strain along the FBG and (b) distribution of the FBG central frequency.

#183098 - $15.00 USD Received 8 Jan 2013; revised 4 Mar 2013; accepted 5 Mar 2013; published 14 Mar 2013

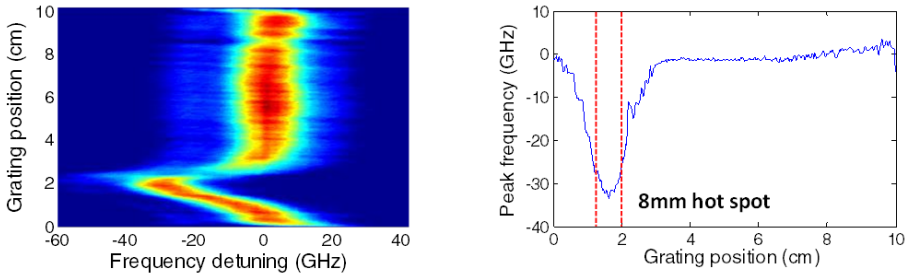

Fig. 6. (a) 3D mapping of the experimental measurements when a 8 mm hot piece of metal is inserted near the beginning of the FBG (b) FBG central frequency distribution.

To test the reliability of this novel sensing configuration, the FBG frequency distribution was successively measured during 2 hours, as shown in Fig. 7(a). Figure 7(b) shows the standard deviation of the FBG frequency calculated as a function of distance. Strong fluctuations were observed at the ends of the grating, possibly caused by the presence of curvature at those positions. However, the central part of the grating shows a high stability in the frequency estimation of about 320 MHz, which corresponds to a temperature accuracy of 0.3 K.

There is a clear and fundamental trade-off between spatial resolution and accuracy on the determination of the grating local frequency (eventually the temperature/strain resolution): even though the FWHM reflection bandwidth of the entire grating is about 1 GHz, the FWHM spectral width of the 20 ps coherent interrogating Gaussian pulse is 22 GHz. It can be clearly observed in Figs. 5-6 that all over this latter spectral width the product between the spectra of the grating and the pulse signal is non-vanishing. As a result a reflected signal will be observed at larger frequency detuning for shorter pulses and the central frequency can be determined with a poorer accuracy. It is remarkable that the local FBG frequency could be determined with a 320 MHz standard deviation, corresponding to 1.5% of the FWHM width of the spectral distribution of the reflected signal. Using these figures our sensing system can produce a normalized accuracy of 0.64 MHz × m; in other words, the local peak reflection frequency can be determined with a 0.64 MHz standard deviation when using a 1 m spatial resolution. Reversely, a temperature resolution of 1 K is secured down to a 0.52 mm spatial resolution, which is an outstanding performance for a distributed fiber sensor, provided that a detection stage with a ~200 GHz sampling capability can be implemented, for instance using all optical sampling. This remains a future prospect albeit with no fundamental physical limitation.

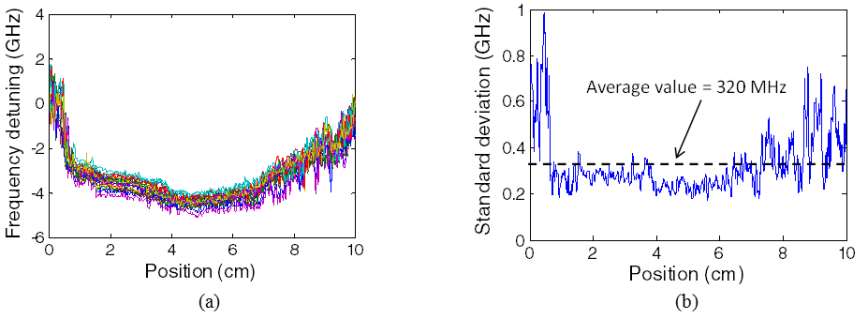

Fig. 7. (a) 20 acquisitions of the grating central frequency distribution when the grating is maintained under constant temperature. (b) Standard deviation of the grating central frequency distribution at room temperature.

#183098 - $15.00 USD Received 8 Jan 2013; revised 4 Mar 2013; accepted 5 Mar 2013; published 14 Mar 2013

It could be also interesting to evaluate the potential distance range of such a distributed sensing system. Actually the reflectivity of the weak FBG must be contained between 2 limits: if the grating shows a too high reflectivity, the interrogating pulse will be severely depleted before reaching the distant end of the FBG and the measurement will be no longer possible. Reversely, if the reflectivity is too low, natural backscattering processes will dominate the distributed reflection signal from the FBG. Inspired by the similarity with the impact of depletion in Brillouin sensors [14], it can be deduced that, in the worst case, the bias in the determination of the peak reflection frequency due to depletion is securely smaller than the measurement standard deviation of 1.5% of the FWHM spectral width if the total grating reflectivity is smaller than 20% [14]. Returning to the standard model for a weak FBG, it can be straightforwardly deduced that such a total reflectivity is reached if the product *linear reflectivity* × *grating length* is equal to 0.96 (here linear reflectivity means amount of reflection per unit length for an infinitesimal distance increment). By comparing with the strongest backscattering process in optical fibers, i.e. Rayleigh scattering, equivalent to a linear reflectivity of 5×10^{-8} m^{-1} at 1550 nm, it can be straightforwardly calculated that a 100 km long FBG can be realized for distributed sensing with a reflection signal 33 dB larger than Rayleigh backscattering. But this 100 km grating must be weak enough to show a total reflectivity smaller than 20%, which is technically extremely challenging, if feasible. The purpose of the demonstration is just to show that there is no fundamental limitation to make kilometer-long sensors using such an approach, i.e. with a distance range comparable to other distributed fiber sensing techniques and with the possibility to still get a comfortable reflection signal. The challenge is now to find a technique to produce extremely long, ideally uniform, FBG showing a very low reflectivity and some recent results demonstrate possible approaches [15]. Note that the 10 cm weak FBG used to make the experimental demonstration already presented a reflectivity in excess of the safe 20%.

4. Tunable delay line

As experimentally demonstrated in Section 3, a limited section of the grating at any preset position along the grating can be spectrally shifted, by locally modifying the grating period. The position of the local modified grating can be simply reconfigured by mechanically moving the perturbation spot. In this situation, an incident pulse at a frequency matching the local shifted peak frequency of the FBG is back-reflected only at that specific position and the reflected pulse returns to the fiber input end with a temporal delay equivalent to the round-trip time of flight, just like a mirror sliding along an optical bench. This is the simple underlying principle for the generation of continuously tunable optical signal delaying.

To validate this concept, a 5 mm-long hot spot at 15 K above room temperature was placed at an arbitrary position along the grating, thereby the resonance spectrum at that position deviates from the spectrum at all other positions by 18 GHz. Then a Gaussian-shaped pulse with FWHM duration of 50 ps was launched into the grating after passing through an optical circulator, as shown in Fig. 4. The reflected pulse was monitored at the reflection port of the circulator using an oscilloscope. Figure 8(a) shows the measured 3D maps of the local FBG reflection spectrum, using the same principle as described in Section 3, while moving the hot spot along the grating. As clearly observed, the spectral distance between the peak reflections of the local grating and of the rest of the grating remains nearly constant, so that a signal centered at the frequency of the local grating will efficiently be reflected. This way a copy of the signal is produced, however with a delay depending on the local grating position. Since the length of the offset grating produced by the hot spot acts as an integration window, it must be kept as short as possible to limit distortion. On the other hand a lower reflection will be produced by a shorter grating, so that there is a clear trade-off between reflectivity and distortion and there is an optimum hot spot dimension for a given signal bandwidth.

#183098 - $15.00 USD Received 8 Jan 2013; revised 4 Mar 2013; accepted 5 Mar 2013; published 14 Mar 2013

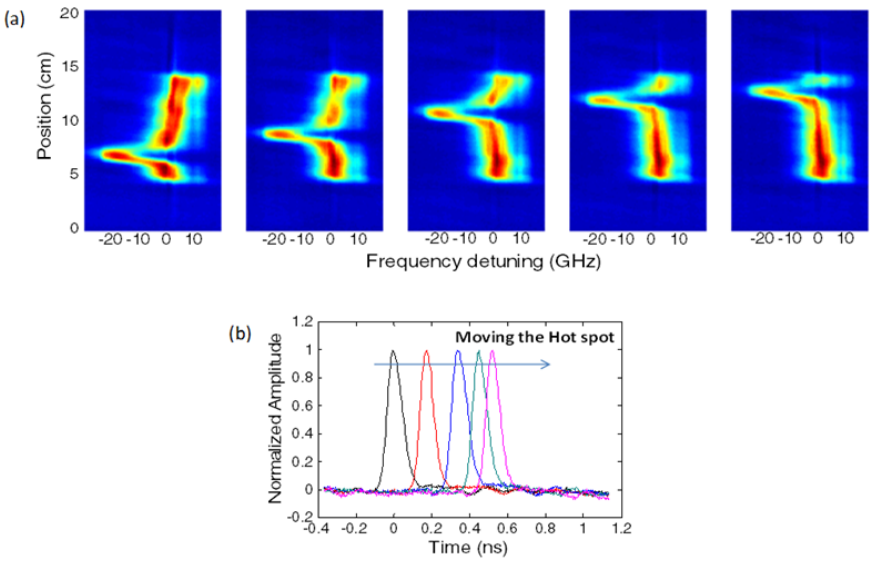

Fig. 8. (a) Spectrogram of the FBG distributed measurement while moving the 5 mm hot spot along the grating. (b) Time waveforms of the delayed signal pulses.

Figure 8(b) shows time traces of the pulse reflection obtained for different grating positions, successfully demonstrating the feasibility of such all-fiber optical signal delaying. The largest time delay achieved in our experiment was 585 ps with a minor signal distortion. However, the maximum achievable time delay is essentially determined by the total length of the grating, so the time delay can be certainly extended up to 1 ns, corresponding to the round-trip propagation along the 10 cm grating.

The amplitude of the reflected signal is essentially given by the physical length of the local grating and the contrast of the refractive index modulation, since they are the key parameters to determine the grating reflectivity. Care must be taken that the spectral shift of local FBG must be large enough, otherwise the spectral overlapping between the signal spectrum and the unmodified FBG spectrum will induce a partial reflection of the incident signal all along the grating length This may cause detrimental interferences and may also degrade the fidelity of the delayed signal in terms of extinction ratio. It must be pointed out that it is no longer strictly required to produce a weak grating for this application, since a large reflection must be ideally produced over a segment of the grating as short as possible and the signal is essentially unperturbed during its propagation along the grating, if the offset frequency is large enough.

5. Conclusions

We have experimentally demonstrated the possibility to measure the local spectral characteristics along a long and weak FBG, using optical time-frequency analysis. A short optical pulse showing duration much shorter than the propagation time through the grating provides the functionality for optical time-domain reflectometry as it propagates through the grating. The time traces obtained by incrementing the interrogating pulse frequency can be readily assembled to obtain a 3D map of the FBG distributed spectrum using a very simple bench-top layout. In principle, the resultant yields all information about the variations in the profile of the refractive index along the long FBG. Due to the high sensitivity of the FBG spectrum to changes in temperature or strain, the proposed measurement system has set the foundation for the development of a novel robust solution for high spatial resolution distributed fiber sensing with no need of optical pumping and sophisticated controlling systems. It has a clear potential in fields like fiber optics assisted surgery, micromechanics

#183098 - $15.00 USD Received 8 Jan 2013; revised 4 Mar 2013; accepted 5 Mar 2013; published 14 Mar 2013

and biosensing. However, such a sensing system is not limited to a short sensing range with a high spatial resolution, as it could be clearly extrapolated, and can also be adapted for longer range with lower spatial resolution. Through a simple estimation we can anticipate that the weak long FBG can perfectly compete with existing distributed fiber sensing solutions, provided that a technological solution can be implemented to produce very long and very weak FBGs in a mass production approach. The 2 illustrating applications shown in this paper support our vision that long weak FBGs have still unveiled functionalities and will be certainly in the future a promising device for various applications.

Acknowledgments

The authors wish to acknowledge the financial support of the European Commission through the COST Action TD1001 "OFSeSa"; Infraestructura FEDER UPVOV08-3E-008, FEDER UPVOV10-3E-492, Ministerio de Ciencia e Innovación through the project TEC2011-29120-C05-05, the Swiss National Science Foundation through project 200021-134546 and the EPFL Space Center.

#183098 - $15.00 USD Received 8 Jan 2013; revised 4 Mar 2013; accepted 5 Mar 2013; published 14 Mar 2013